18th International Conference on Information Fusion
Washington, DC - July 6-9, 2015

Multi-Target Tracking for Multistatic Sonobuoy Systems

Mark Morelande*, Sofia Suvorova*, Fiona Fletcher†, Sergey Simakov†, Bill Moran‡

***Abstract*—We describe a technique for detection and tracking of multiple targets using a multistatic sonobuoy array. The innovation in the proposed algorithm is the use of a clustering step, posed as Bayesian mixture estimation, to produce Cartesian position measurements. These are passed to a sequential Monte Carlo approximation of the multiple hypothesis tracker. The improvement offered by the proposed algorithm compared to an existing algorithm is demonstrated in a simulation analysis.**

I. Introduction

Detection and tracking of underwater targets using a field of active sonobuoys has recently attracted significant research interest [1], [2], [3], [4], [5], [6]. This problem involves determining the number of targets in the area covered by the sonobuoy field and tracking their positions. Measurements of the targets are obtained by the transmission of a signal (a "ping") from a single source (sonobuoy), and collection of reflected measurements at a number of nearby receivers. Difficulties arise because of the low detection probability in an underwater environment and the non-linear relationship between the available position measurements, which are typically in polar coordinates, and the target state.

In [5] a Gaussian mixture approximation of the iterator-corrector version of the CPHDF was proposed for target detection and tracking and, based on this algorithm, a transmitter scheduling algorithm was described. A rudimentary technique for accounting for battery life constraints using a discount factor was also proposed. The prime focus of this paper is on the multitarget tracking problem in the multistatic sonobuoy context.

The cardinalised probability hypothesis density filter (CPHDF) [7] has been used in several papers for tracking in multistatic sonobuoy systems [1], [3], [5]. The CPHDF, which is developed in the random finite set (RFS) framework, approximates the full multi-target posterior density by its first-order moment and a cardinality, or target number, distribution. Although the CPHDF performs well in some scenarios, it has several shortcomings that make its use problematic for tracking using a sonobuoy field. The first weakness is that the exact multiple sensor CPHDF recursion is intractable [8]. This is addressed using a Gaussian mixture approximation of the iterated-corrector version of the CPHDF in [5]. Another undesirable property arising with the iterator-corrector CPHDF is that the result is dependent on the order in which the receiver returns are processed, although often in practise this dependence is not significant.

These deficiencies have motivated the use of a new approach based on the use of clustering as a pre-processing step to accentuate target measurements and mitigate clutter. The clustering step produces Cartesian position "measurements" which are then used in a sequential Monte Carlo implementation of the MHT. This approach has been used, for instance, in [3], [9]. A challenge here is to perform clustering with polar position measurements, each referenced to a different set of axes.

Of more concern, is the effect identified in [10] whereby a missed target detection causes the mass associated with a tracked target to be distributed elsewhere in the state space causing the track to be lost. This is particularly problematic in sonobuoy tracking where the detection probability is quite low and only a fraction of the surveillance area can be observed from a single ping. Particle filters (PFs) have been used for approximation of the full multi-target posterior density in [2]. While offering asymptotically optimal inference, PFs generally require considerable computational resources.

We propose a new approach in which a clustering pre-processing step is used to accentuate target measurements and remove clutter measurements. We develop a Bayesian mixture estimation algorithm for forming clusters in Cartesian coordinates of non-linear position measurements collected across the sonobuoy field. The proposed algorithm does not require *a priori* knowledge of the number of clusters. The Cartesian position "measurements" supplied by the mixture estimator are used in a sequential Monte Carlo (SMC) implementation of the multiple hypothesis tracker (MHT). Only the association hypotheses are sampled using a procedure with polynomial expense in the number of targets. Because the clustering step removes most of the clutter measurements the SMC-MHT performs well with a small sample size so that good performance can be achieved with moderate expense.

The use of a pre-processing step is similar to the approaches of [3], [6]. However, in [3], the clustering step is performed on a grid, preventing separation of closely-spaced targets and tracking is performed using the CPHDF, the shortcomings of which are discussed above. In [4] clustering and tracking are performed using two PFs operating on the single target state space. This is computationally expensive and suboptimal because it involves estimating states of multiple targets in a single target state space.

The measurement model is developed in Section II. The clustering algorithm is described in Section III and used as part of a sequential Monte Carlo approximation of the MHT described in Section IV. Simulations reported in Section V show considerable improvement over the iterated-corrector Gaussian mixture CPHDF at much reduced computational expense.

II. Measurement Modelling

A multistatic sonar system with s sources and d receivers dispersed across a search area is considered. Let $\boldsymbol{\xi}_i \in \mathbb{R}^2$, $i = 1,\ldots,s$ denote the position of the ith source and $\boldsymbol{\xi}_{i+s} \in \mathbb{R}^2$, $i = 1,\ldots,d$ denote the position of the ith receiver.

Individual sonobuoys comprise an underwater section consisting of transducers (emitters) and hydrophones (receivers), connected to a float containing RF communications and other equipment, including possibly GPS equipment.

Consider a target with state $\boldsymbol{x} = (\boldsymbol{p}', \dot{\boldsymbol{p}}')'$ where $\boldsymbol{p} = (x, y)'$ is target position and $\dot{\boldsymbol{p}} = (\dot{x}, \dot{y})'$ is target velocity. The measurement at the jth receiver resulting from a ping from the ith source comprises the bistatic range from source to target to receiver and the angle from the target to the receiver, for all transmitted waveforms. The measurement vector $\boldsymbol{z}$ satisfies

$$\boldsymbol{z}|\boldsymbol{x} \sim \mathsf{N}(\boldsymbol{h}_j(\boldsymbol{x}), \boldsymbol{R}_j) \tag{1}$$

where the measurement function $\boldsymbol{h}_j(\cdot)$ is

$$\boldsymbol{h}_j(\boldsymbol{x}) = \begin{bmatrix} |\boldsymbol{p} - \boldsymbol{\xi}_i| + |\boldsymbol{p} - \boldsymbol{\xi}_{s+j}| \\ \angle(\boldsymbol{p} - \boldsymbol{\xi}_{s+j}) \end{bmatrix}, \tag{2}$$

where $\angle(\boldsymbol{u})$ is the angle between $\boldsymbol{u}$ and the x-axis of the reference coordinate system. Note that only Doppler insensitive waveforms are considered here.

The target detection process is modelled using signal excess component data stored in look up tables depending on waveforms, source, receiver and target depths and source-receiver separation distance. The SNR calculation employs precomputed data sets of the Signal Excess components, namely (a) Target Echoes (TE0) for a standard target with an isotropic 0 dB Target Strength, and (b) Reverberation Levels (RL). Computation of the TE0 and RL data was carried out offline using the Gaussian ray bundle eigenray propagation model [11], [12]. Let $\overline{\mathrm{SE}}$ denote the mean signal excess returned from the look-up table for a given configuration of source, receiver and target. The TE0 and RL data were calculated for a set of waveforms, different sonar depth settings and a range of source-receiver separation distances. The instantaneous signal excess is assumed to satisfy $\mathrm{SE} \sim \mathsf{N}(\cdot; \overline{\mathrm{SE}}, \sigma^2)$. The mean Signal Excess $\overline{\mathrm{SE}}$ was calculated using the following form of the sonar equation:

$$\overline{\mathrm{SE}} = \mathrm{TE0} + \mathrm{TS} - 10\log_{10}(10^{\mathrm{RL}/10} + 10^{\mathrm{NL}/10}) - \mathrm{DT}, \tag{3}$$

where TS is the bistatic Target Strength obtained from the associated TS table for a given bistatic geometry, NL is noise level after beamforming, DT is a detection threshold given by the equation, $\mathrm{DT} = 10\log_{10}\left(\frac{\mathrm{erfcinv}^2(2P_{\mathrm{fa}})}{B\tau}\right)$, in which B is bandwidth, τ is pulse length, P_{fa} is the probability of false alarms. The dB form of the SNR is obtained from SE as follows: $\mathrm{SNR}_{\mathrm{dB}} = \mathrm{SE} + \mathrm{DT}$.

For a given pulse, the resulting SNR value defines the mean of the unit-variance normal distribution of the emulated receiver detection statistic. We sample from this distribution and if the sample value exceeds a P_{fa}-dependent threshold, we declare a detection. False alarms are produced on a grid determined by the beamwidth and range resolution of the receiver. The mean signal excess also allowed calculation of the probability of detection for a target in any location. The measurement generation process is described in more detail in [5].

III. Clustering of polar position measurements

We employ a clustering pre-processor, posed as a Bayesian mixture estimation problem, to produce a set of target-originated position measurements in Cartesian coordinates. The algorithm requires only an upper bound on the number of clusters. We begin by describing the mixture estimation procedure and then demonstrate its performance in a simulation scenario.

A. Bayesian mixture estimation

Let $\boldsymbol{z}_1,\ldots,\boldsymbol{z}_m$ denote the polar position measurements from all sensors with corresponding measurement noise covariance matrices $\boldsymbol{R}_1,\ldots,\boldsymbol{R}_m$. Suppose at most $\bar{q}$ clusters and let $\omega_j \in \{0,\ldots,\bar{q}\}$ denote the cluster assigned to the jth measurement with $\omega_j = 0$ indicating that the jth measurement is not assigned to any cluster. The clusters are characterised by the weights $w_0,\ldots,w_{\bar{q}}$ and locations $\boldsymbol{\mu}_1,\ldots,\boldsymbol{\mu}_{\bar{q}}$ in Cartesian coordinates. The spread of points in a cluster is determined by the known measurement noise covariance matrices. Only the locations, collected into $\boldsymbol{\theta} = [\boldsymbol{\mu}_1',\ldots,\boldsymbol{\mu}_{\bar{q}}']'$, are assumed unknown. Adopting a Bayesian approach, we aim to compute the posterior density,

$$p(\boldsymbol{\theta}|\boldsymbol{z}_{1:m}) \propto \sum_{i_1,\ldots,i_m=0}^{\bar{q}} \prod_{j=1}^{m} p(\boldsymbol{z}_j|\boldsymbol{\theta}, \omega_j = i_j)\, \pi_0(\boldsymbol{\theta}) \tag{4}$$

where $\pi_0(\cdot)$ is a prior for the location parameters. Equation (4) shows that the computation of the posterior density requires the evaluation of $(\bar{q}+1)^m$ hypotheses regarding the placement of measurements into clusters. This is clearly infeasible for any reasonable values of $\bar{q}$ and m. As in [9], [13] we adopt an approximate method based on sequential processing of the measurements. In addition to enabling computationally efficient approximation of the posterior, sequential processing avoids the lack of identifiability which leads to the label switching problem [14].

Details of the sequential mixture estimation algorithm can be found in [9]. The main difference between the clustering problem considered here and that of [9] is that here the polar position measurements are a nonlinear function of the cluster means, which are in Cartesian coordinates. As a result the weights and conditional parameter densities

encountered during the sequential processing procedure cannot be found in closed-form. We find an accurate approximations using a progressive Monte Carlo scheme, as described in [15]. This involves decomposing the likelihood into a product of terms and processing each term in sequence. After all terms have been processed, the required integrals can be approximated and moment-matched Gaussian approximations to the conditional parameter densities obtained.

On completion of the processing of all measurements, the clusters in the most probable hypothesis sequence are used to form Cartesian position measurements which are passed to the tracking algorithm. Of the clusters found in this hypothesis only those with at least $\underline{d}$ measurements assigned to them are used in the tracking algorithm.

The required measurement noise covariance matrix, detection probability and clutter density of the "effective sensor" are found via simulation, as described in the following section.

B. Simulation results

The performance of the sequential mixture estimation algorithm is demonstrated on the scenario of Figure 2. The scenario contains 64 collocated sources and receivers arranged on a regular 8×8 grid with 5 km spacing between adjacent grid points. The signal is transmitted from a single source located at $(15,15)$ km. The target depth is 80m. Only clusters assigned at least $\underline{d}=3$ polar measurements are returned as "effective measurements".

The detection probability at each target location is found over 50 realisations for a Doppler insensitive waveform. The pruning step in the algorithm limits the number of label sequences to 100. The detection probability and the base-10 logarithm of the determinant of the sample covariance matrix of the target position estimate are plotted against target position in Figure 1. In the latter plot the black pixels correspond to target positions with detection probabilities less than 0.1. The mixture estimation algorithm provides detection probabilities close to one and accurate effective measurements for many target positions, even those which are distant from the pinging source. Importantly, these results are achieved with an effective clutter density of only 2.7×10^{-4} clutter measurements per scan per m^2.

The detection probabilities and covariance matrices shown in Figure 1 are used to calculate the detection probability for the tracking algorithm described in Section IV. Linear interpolation is used to interpolate between the grid points.

IV. Multiple hypothesis tracking algorithm

Tracking using the Cartesian position "measurements" provided by the mixture estimation algorithm is performed using a sequential Monte Carlo (SMC) approximation to the multiple hypothesis tracker (MHT), similar to that described in [9]. The tracking model and algorithm are described in this section.

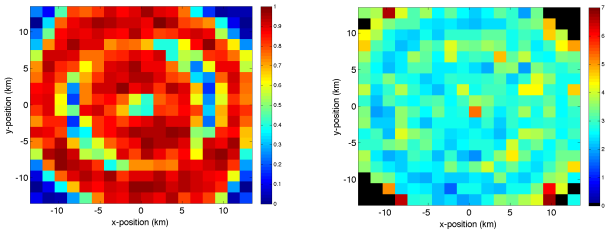

(a) Detection probability (b) Covariance matrix

Fig. 1. Performance of the mixture estimation algorithm: (a) detection probability and (b) determinant of covariance matrix plotted against target position relative to the transmitter position.

A. Modelling

Measurements returned by the pre-processing mixture estimation algorithm can be associated with existing targets or new targets. Existing targets persist from one scan to the next with probability ϱ and evolve according to

$$\boldsymbol{x}_t|\boldsymbol{x}_{t-1} \sim \mathsf{N}(\cdot;\boldsymbol{F}\boldsymbol{x}_{t-1},\boldsymbol{Q}) \tag{5}$$

where

$$\boldsymbol{F}=\begin{bmatrix}1 & T\\ 0 & 1\end{bmatrix}\otimes \boldsymbol{I}_2 \tag{6}$$

$$\boldsymbol{Q}=q\begin{bmatrix}T^3/2 & T^2/2\\ T^2/2 & T\end{bmatrix}\otimes \boldsymbol{I}_2. \tag{7}$$

In each scan there are g possible new targets. The ath new target is born with probability κ_a and has prior density $\mathsf{N}(\cdot;\hat{\boldsymbol{x}}_{0,a},\boldsymbol{P}_{0,a})$.

The Cartesian position measurements obtained by the mixture estimation algorithm are collected into the vector $\boldsymbol{Y}_t=[\boldsymbol{y}'_{t,1},\ldots,\boldsymbol{y}'_{t,m_t}]'$, where m_t is the number of measurements. Let r_{t-1} denote the number of existing targets at time $t-1$. The vector $\boldsymbol{\vartheta}_t=[\vartheta_{t,1},\ldots,\vartheta_{t,r_{t-1}+g}]'$ where $\vartheta_{t,i}\in\{0,\ldots,m_t+1\}$, associates existing and new targets with the available measurements. For $i=1,\ldots,r_{t-1}$, $\vartheta_{t,i}=j\leq m_t$ means that the ith target survives and is associated with the jth measurement, $\vartheta_{t,i}=0$ means that the ith target survives but is not detected and $\vartheta_{t,i}=m_t+1$ means the ith target no longer exists. The association $\vartheta_{t,a+r_{t-1}}$ for the ath potential new target, $a=1,\ldots,g$, is similarly defined.

When pinged by the cth source a target with state $\boldsymbol{x}$ produces a measurement with probability $\eta(c,\boldsymbol{x})$. The target-originated measurement is assumed to be distributed as $\mathsf{N}(\cdot;\boldsymbol{H}\boldsymbol{x},\boldsymbol{R}(c,\boldsymbol{x}))$ where $\boldsymbol{H}$ selects the position elements of the state and $\boldsymbol{R}(c,\boldsymbol{x})$ is measurement noise covariance matrix. False, or clutter, measurements are assumed to follow a Poisson process with uniform density λ. The measurement covariance matrix, detection probability and clutter density are found via Monte Carlo simulation, as in Section III-B.

B. Sequential Monte Carlo approximation

In principle, the MHT calls for enumeration and evaluation of all possible association hypotheses. It is well

known that exact implementation of the MHT is impractical because of the exponential number of possible target existence hypotheses and assignment of measurements to targets. We address this problem by using an asymptotically exact SMC approximation. The approach differs slightly from that proposed in [9] because of the manner in which target birth and death are handled in the process model. Here, a new target can be born even if it isn't detected. This is necessary because the sensor field isn't able to view the whole surveillance area by pinging a single source.

Let $\boldsymbol{\vartheta}_{1:t-1}$ denote a sequence of association hypothesis vectors. In the SMC-MHT the posterior at time $t-1$ is represented by the samples $\boldsymbol{\vartheta}^1_{1:t-1},\ldots,\boldsymbol{\vartheta}^n_{1:t-1}$ with corresponding weights $w^1_{t-1},\ldots,w^n_{t-1}$, where n is the sample size. The posterior probability of the sequence $\boldsymbol{\vartheta}_{1:t-1}$ is approximated as

$$\mathsf{P}(\boldsymbol{\vartheta}_{1:t-1}|\boldsymbol{Y}_{1:t-1}) \approx \sum_{\{a:\boldsymbol{\vartheta}^a_{1:t-1}=\boldsymbol{\vartheta}_{1:t-1}\}} w^a_{t-1} \tag{8}$$

The posterior densities of the targets existing under $\boldsymbol{\vartheta}^a_{1:t-1}$ are approximated by Gaussians. The posterior mean and covariance matrix of the ith target under $\boldsymbol{\vartheta}^a_{1:t-1}$ are $\hat{\boldsymbol{x}}^a_{i,t-1|t-1}$ and $\boldsymbol{P}^a_{i,t-1|t-1}$, respectively.

Given the measurements $\boldsymbol{Y}_t$ it is desired to draw samples of $\boldsymbol{\vartheta}_{1:t}$. This is done by appending samples of the current hypothesis vector $\boldsymbol{\vartheta}_t$ to the previously sampled sequences of hypothesis vectors. We first select the samples $\boldsymbol{\vartheta}^1_{1:t-1},\ldots,\boldsymbol{\vartheta}^n_{1:t-1}$ which will be used to make up the t-length hypothesis vector samples. The indices $a(1),\ldots,a(n)$ of the samples to be used are selected such that $\mathsf{P}(a(k)=b)=w^b_{t-1}$. This is equivalent to the resampling step [16] which is used to mitigate sample degeneracy.

For $k=1,\ldots,n$, $\boldsymbol{\vartheta}^k_t \in \{0,\ldots,m_t+1\}^{z^k_t}$ where $z^k_t = r^{a(k)}_{t-1}+g$ with r^a_{t-1} the number of targets existing under $\boldsymbol{\vartheta}^a_{1:t-1}$. The meaning of the values taken by the elements of $\boldsymbol{\vartheta}^k_t$ has been discussed above. Only values of $\boldsymbol{\vartheta}^k_t$ in which each measurement is assigned to at most one target are valid. Let $V^k \subset \{0,\ldots,m_t+1\}^{z^k_t}$ denote the set of valid hypothesis vectors. Then, the probability of $\boldsymbol{\vartheta}^k_t \in V^k$ is

$$\mathsf{P}(\boldsymbol{\vartheta}^k_t) \propto \prod_{i=1}^{z^k_t} \psi_{i,\vartheta^k_{t,i}} \tag{9}$$

where

$$\psi^k_{i,j} = \begin{cases} u_i \xi^{a(k)}_{0,i}, & j=0, \\ u_i \xi^{a(k)}_{j,i}/\lambda, & j=1,\ldots,m_t, \\ 1-u_i, & j=m_t+1 \end{cases} \tag{10}$$

The quantity $\xi^a_{0,i}$ is the weight attached to non-detection of the ith target of the ath particle and depends on the detection probability and the prior target state density. This tends to increase as the detection probability decreases. For $j=1,\ldots,m_t$ the quantity $\xi^a_{j,i}$ is the association strength between the jth measurement and the ith target of the ath sample. This depends on the measurement, the conditional measurement density, the detection probability and the prior target state density.

It is not feasible to draw samples of the hypothesis vector directly from (9) because the number of elements in V^k increases exponentially with the numbers of targets and measurements. Instead we draw from an importance distribution $\mathsf{Q}(\cdot)$ which factorises so that elements of the hypothesis vector can be drawn sequentially. Let $\boldsymbol{\vartheta}^k_{t,1:i}$ denote the first i elements of the hypothesis vector $\boldsymbol{\vartheta}^k_t$ and define the set

$$A_i(\boldsymbol{\vartheta}^k_{t,1:i-1}) = \{0,\ldots,m_t+1\} \backslash \{\vartheta^k_{t,b},\, b=1,\ldots,i-1 : \vartheta^k_{t,b} \in \{1,\ldots,m_t\}\} \tag{11}$$

The set $A_i(\boldsymbol{\vartheta}^k_{t,1:i-1})$ contains the hypotheses available for the ith element of the hypothesis vector. The importance distribution is

$$\mathsf{Q}(\boldsymbol{\vartheta}^k_t) = \prod_{i=1}^{z^k_t} \frac{\psi_{i,\vartheta^k_{t,i}}}{\sum_{b\in A_i(\boldsymbol{\vartheta}^k_{t,1:i-1})} \psi_{i,b}} \tag{12}$$

The weight assigned to the sample $\boldsymbol{\vartheta}^k_t$ drawn from the importance distribution (12) is

$$w^k_t \propto \frac{\mathsf{P}(\boldsymbol{\vartheta}^k_t)}{\mathsf{Q}(\boldsymbol{\vartheta}^k_t)} = \prod_{i=1}^{z^k_t} \sum_{b\in A_i(\boldsymbol{\vartheta}^k_{t,1:i-1})} \psi_{i,b} \tag{13}$$

The t-length hypothesis vector sequence for the kth sample is constructed as $\boldsymbol{\vartheta}^k_{1:t} = [\boldsymbol{\vartheta}^{a(k)}_{1:t-1}, \boldsymbol{\vartheta}^k_t]$. We require the posterior densities of the targets existing under each sampled hypothesis vector. The posterior density of the ith surviving target under $\vartheta^k_{t,i}=j$ is given by

$$p(\boldsymbol{x}_{i,t}|\boldsymbol{\vartheta}^k_{1:t}, \boldsymbol{Y}_{1:t}) \propto \begin{cases} [1-\eta(c_t,\boldsymbol{x})] & \\ \quad \times \mathsf{N}(\boldsymbol{x}_{i,t}; \hat{\boldsymbol{x}}^{a(k)}_{i,t|t-1}, \boldsymbol{P}^{a(k)}_{i,t|t-1}), & j=0, \\ \eta(c_t,\boldsymbol{x})\mathsf{N}(\boldsymbol{y}_{t,j}; \boldsymbol{H}\boldsymbol{x}, \boldsymbol{R}(c_t,\boldsymbol{x})) & \\ \quad \times \mathsf{N}(\boldsymbol{x}_{i,t}; \hat{\boldsymbol{x}}^{a(k)}_{i,t|t-1}, \boldsymbol{P}^{a(k)}_{i,t|t-1}), & j=1,\ldots,m_t. \end{cases} \tag{14}$$

where c_t is the index of the pinging source for the tth scan. Similar expressions hold for the birth targets.

Note that the association strengths appearing in (10) and the densities (14) can't be found in closed-form because of state-dependent detection probabilities and measurement covariance matrices. The first approximation is to evaluate the measurement covariance matrix at the prior mean of the state. This allows the conditional measurement density and the prior state density to be combined. The detection probability is then evaluated at the corrected value of the state. Thus, we have

$$\begin{aligned} \eta(\boldsymbol{x})\mathsf{N}(\boldsymbol{y},\boldsymbol{H}\boldsymbol{x},\boldsymbol{R}(\boldsymbol{x}))\mathsf{N}(\boldsymbol{x};\hat{\boldsymbol{x}}_0,\boldsymbol{P}_0) &\approx \eta(\boldsymbol{x})\mathsf{N}(\boldsymbol{y},\boldsymbol{H}\boldsymbol{x},\boldsymbol{R}(\hat{\boldsymbol{x}}_0))\mathsf{N}(\boldsymbol{x};\hat{\boldsymbol{x}}_0,\boldsymbol{P}_0) \\ &= \eta(\boldsymbol{x})\mathsf{N}(\boldsymbol{y};\hat{\boldsymbol{y}},\boldsymbol{S})\mathsf{N}(\boldsymbol{x};\hat{\boldsymbol{x}},\boldsymbol{P}) \qquad (15) \\ &\approx \eta(\hat{\boldsymbol{x}})\mathsf{N}(\boldsymbol{y};\hat{\boldsymbol{y}},\boldsymbol{S})\mathsf{N}(\boldsymbol{x};\hat{\boldsymbol{x}},\boldsymbol{P}) \qquad (16) \end{aligned}$$

Eq. (15) follows from the Gaussian product formula [17]. We obtain Gaussian approximations by evaluating the measurement covariance matrix at the prior mean of the state. Then, the detection probabilities are evaluated.

V. Simulation Results

In this section, the proposed SMC-MHT is compared with the GM-CPHD iterated-corrector approximation proposed in [5] for the scenario shown in Figure 2. This small scenario contains 64 collocated sources and receivers arranged on a regular 8×8 grid with 5 km spacing. Three targets move in the sonobuoy field. One begins outside the sonobuoy field and moves into it. The target trajectories are shown in Figure 2. The targets are observed for a period of 60 min at intervals of $T = 30$ s.

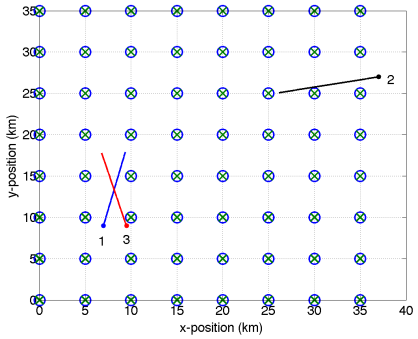

Fig. 2. Simulation scenario for tracking with sources (blue circles), receivers (green crosses) and target trajectories.

At each scan it is necessary to select a source to ping. At the tth scan we select the source with the highest expected number of detections of target $(t \bmod 3)+1$. Because target 2 is far from targets 1 and 3 it is unlikely that detections of target 2 will be received when pinging for targets 1 and 3 and *vice versa*. This clairvoyant scheme is clearly not feasible in practice, since it requires knowledge of the target position, but is used here because the focus of this paper is on tracking performance rather than scheduling. An approach to source scheduling in the absence of target position information was proposed in [5], and we will return to the topic in later publications. Both tracking algorithms require the selection of a number of parameters. These are summarised in Table I.

TABLE I
Algorithm parameters

Parameter	Algorithm	
	SMC-MHT	GM-CPHD
Mixture estimation		
Pruning length	100	–
Integration sample size	250	–
Tracking		
Hypothesis sample size	20	50
Integration sample size	–	1000
Birth densities	100	225

The performance of the algorithm is measured by the mean optimal subpattern assignment OSPA [18] averaged over 50 realisations. The OSPA distance between two sets $X = \{\boldsymbol{x}_1, \ldots, \boldsymbol{x}_m\}$ and $Y = \{\boldsymbol{y}_1, \ldots, \boldsymbol{y}_n\}$, $n \geq m$, is defined as

$$d(X,Y) = \left(1/n \min_{\pi \in \Pi_n} \sum_{i=1}^{m} \min\left\{ \|\boldsymbol{x}_i - \boldsymbol{y}_{\pi(i)}\|, c \right\}^p + c^p (n-m) \right)^{1/p} \tag{17}$$

where Π_n is the set of permutations of the integers $1, \ldots, n$ and c and p are pre-defined constants. This metric is widely used as a measure of performance in RFS (See, for instance, [19] §2.4). In this analysis we use $p = 2$ and $c = 100$. Note that the OSPA metric penalises errors in estimation of both the number of targets and their states.The results are shown in Figure 3. The SMC-MHT is seen to perform much better than the GM-CPHD iterated-corrector. The difference appears to be mainly in the ability of the SMC-MHT to reliably maintain track. This improved performance is achieved with about 1/3 the computational expense of the GM-CPHD iterator-corrector, as measured by the run time of Matlab implementations. The extremely poor performance of the GM-CPHDF iterated-corrector can be attributed, in this instance, to the low detection probability and, in particular, the fact that it cannot be expected to detect all targets by pinging a single source. For instance, in this scenario, target 2 can only be reliably observed every three scans.

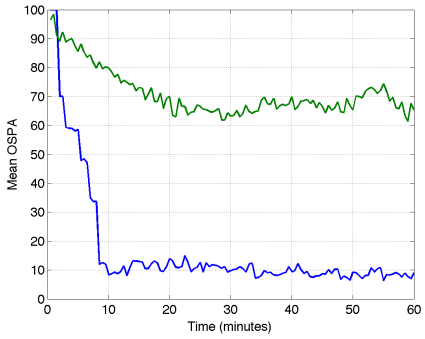

Fig. 3. Mean OSPA plotted against time for the SMC-MHT with clustering (blue) and the GM-CPHD iterator corrector (green).

VI. Conclusions

In this paper, we have proposed a sequential Monte Carlo approximation of the multiple hypothesis tracker for multi-target detection and tracking with application in multistatic sonar fields using a Gaussian mixture approximation and compared it numerically to the cardinalised probability hypothesis density filter of Mahler. A key feature is the use of clustering on the measurements obtained from the sonobuoy field prior to tracking in place of a previously implemented iterator-corrector method thus overcoming the dependence on order of processing of measurements. By accentuating target-originated measurements and removing clutter measurements this approach greatly reduces the difficulties associated with the tracking problem. The

proposed approach offered both improved performance and reduced computational expense compared to the cardinalised probability hypothesis density filter.

Currently being explored are several possible directions for future work including the incorporation of sonobuoy drift, manoeuvring targets, and sophisticated source scheduling that allows for multiple simultaneous transmitters and realistic battery life constraints.

REFERENCES

[1] O. Erdinc, P. Willett, and S. Coraluppi, "The Gaussian mixture cardinalized PHD tracker on MSTWG and SEABAR'07 datasets," in *Proceedings of the International Conference on Information Fusion*, Cologne, Germany, 2008.

[2] F. Fletcher and S. Arulampalam, "A comparison of existence-based multitarget trackers for multistatic sonar," in *Proceedings of the International Conference on Information Fusion*, Singapore, 2012.

[3] R. Georgescu and P. Willett, "The GM-CPHD tracker applied to real and realistic multistatic sonar data sets," *IEEE Journal of Oceanic Engineering*, vol. 37, no. 2, pp. 220–235, 2012.

[4] J. Georgy, A. Noureldin, and G.R. Mellema, "Clustered mixture particle filter for underwater multitarget tracking in multistatic active sonobuoy systems," *IEEE Transactions on Systems, Man and Cybernetics, Part C*, vol. 42, no. 4, pp. 547–560, 2012.

[5] S. Suvorova, M. Morelande, B. Moran, S. Simakov, and F. Fletcher, "Ping scheduling for multistatic sonar systems," in *Proceedings of the International Conference on Information Fusion*, 2014.

[6] K. Wilkens and M. Daun, "A Gaussian mixture motion model and contact fusion applied to the Metron data set," in *Proceedings of the International Conference on Information Fusion*, Chicago, USA, 2011.

[7] R.P.S. Mahler, "PHD filters of higher order in target number," *IEEE Transactions on Aerospace and Electronic Systems*, vol. 43, no. 3, pp. 1523–1543, 2007.

[8] R. Mahler, "The multisensor PHD, I: General solution via multitarget calculus," in *Proceedings of SPIE*, 2009, vol. 7336.

[9] M. Morelande and N. Gordon, "Comparison of fusion methods for multiple target tracking," in *Proceedings of the International Conference on Information Fusion*, Edinburgh, Great Britian, 2010.

[10] D. Fränken, M. Schmidt, and M. Ulmke, ""Spooky action at a distance" in the cardinalised probability hypothesis density filter," *IEEE Transaction on Aerospace and Electronic Systems*, vol. 45, no. 4, pp. 1657–1664, 2009.

[11] Henry Weinberg and Ruth Eta Keenan, "Gaussian ray bundles for modeling high-frequency propagation loss under shallow-water conditions," *The Journal of the Acoustical Society of America*, vol. 100, no. 3, pp. 1421–1431, 1996.

[12] R.E. Keenan, "An introduction to grab eigenrays and cass reverberation and signal excess," in *OCEANS 2000 MTS/IEEE Conference and Exhibition*, 2000, vol. 2, pp. 1065–1070 vol.2.

[13] N. Chopin, "Inference and model choice for sequentially ordered hidden Markov models," *Journal of the Royal Statistical Society, Series B*, vol. 69, no. 2, pp. 269–284, 2007.

[14] M. Stephens, "Dealing with label switching in mixture models," *Journal of the Royal Statistical Society, Series B*, vol. 62, no. 4, pp. 795–809, 2000.

[15] M.R. Morelande and B. Ristic, "Radiological source detection and localisation using Bayesian techniques," *IEEE Transactions on Signal Processing*, vol. 57, no. 11, pp. 4220–4231, 2009.

[16] N.J. Gordon, D.J. Salmond, and A.F.M. Smith, "Novel approach to nonlinear/non-Gaussian Bayesian state estimation," *IEE Proceedings Part F*, vol. 140, no. 2, pp. 107–113, 1993.

[17] Y.C. Ho and R.C.K. Lee, "A Bayesian approach to problems in stochastic estimation and control," *IEEE Transactions on Automatic Control*, vol. 9, pp. 333–339, 1964.

[18] D. Schuhmacher, B-T. Vo, and B-N. Vo, "A consistent metric for performance evaluation of multi-object filters," *IEEE Transactions on Signal Processing*, vol. 56, no. 8, pp. 3447–3457, 2008.

[19] B. Ristic, *Particle Filters for Random Set Models*, SpringerLink : Bücher. Springer, 2013.